Investigating the multi-layered Richtmyer-Meshkov instability with high-order accurate numerical methods

Marc T. Henry de Frahan[1], **Pooya Movahed**[1], **and Eric Johnsen**[1]

1 Introduction

The Richtmyer-Meshkov instability (RMI) occurs in flows where a shock interacts with a perturbed interface between two different fluids. At the interface, the interacting shock deposits baroclinic vorticity that drives the perturbation growth [1]. Conducting theoretical and experimental analysis is important to understand the physics of the RMI and its role in the context of high-energy-density physics [3], particularly inertial confinement fusion [8] and supernova collapse [6]. In these latter problems, the geometry is such that the shock interacts with multiple layers of materials. Thus, the multi-layered RMI is particularly relevant in these multi-material problems, where an accurate characterization of the level of mixing is important. Although the single interface RMI has been studied extensively in the past, through both experiments [2] and numerical simulations [5, 7], little attention has been given to the multi-layered RMI.

Using conservative, non-oscillatory, and high-order accurate methods to solve the multifluid equations of motion [9, 4], we study the multi-layered RMI to better understand the physics of shocks interacting with several perturbed fluid interfaces and the influence these instabilities have on each other. We present preliminary numerical simulations of the two-layered RMI. This instability can be described as three adjacent fluids with initially perturbed interfaces. The RMI is caused by a shock, initialized upstream, sequentially impinging on these interfaces. We vary several parameters and study their effect on the RMI development to characterize the fluid mixing as a function of time. Using two-dimensional simulations, we analyze the effects of the shocks and rarefactions and the types of fluid and their thickness on the mixing between the three fluids. We characterize the effect of the second instability on the growth rate of the first one and compare to that of the traditional single-layered RMI growth.

Mechanical Engineering Department, University of Michigan
Ann Arbor, MI 48109 (USA)

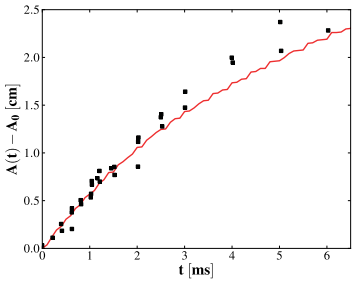

Fig. 1 Instability growth vs time. Black squares: experimental data from [2]. Solid red line: simulation results.

2 Single-layered RMI Validations

We use the single-layered RMI experiment from [2] to validate our numerical methods. The parameters for the cases we consider in this paper are presented in Table 1. A shock initialized in air impinges a perturbed interface between the air and a denser gas, SF_6, thereby initiating the RMI growth. The early-time growth of the instability (before reshock) from the simulation agrees with the experimental data, Figure 1.

3 Multi-layered RMI

Our setup for the multi-layered RMI can be described as three adjacent gases (A, B, and C) separated by initially perturbed interfaces and a shock initialized in the first gas, Figure 2. To compare with previous single-layered RMI studies, we choose air for gas A, SF_6 for gas B, and a shock Mach number of 1.21. We study the effect of increasing the distance separating gas A from gas C, i.e. increasing the thickness of gas B, measured with the non-dimensional distance $\frac{h}{\lambda}$, where λ is the perturbation wavelength. We also change the density of gas C to create either a

Table 1 For all cases: $M_s = 1.21$ in the air, $p_{atm} = 10^5$Pa, $\rho_{air} = 1.351\,\text{kg/m}^3$, $\gamma_{air} = 1.276$, $M_{air} = 34.76\,\text{kg/kmol}$, $\rho_{SF_6} = 5.494\,\text{kg/m}^3$, $\gamma_{SF_6} = 1.093$, $M_{SF_6} = 146.05\,\text{kg/kmol}$, $A = 0.183$cm, and $\lambda = 5.933$cm. Relevant properties for gas C:

Case	gas A	gas B	ρ_C [kg/m^3]	γ_C	M_C [kg/kmol]
nominal [2]	air	SF_6	-	-	-
1	air	SF_6	0.178	5/3	4
2	air	SF_6	10	5/3	300

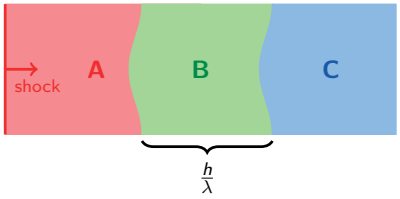

Fig. 2 Multi-layered RMI setup.

reflected rarefaction or shock at the second interface. The nominal case (no gas C) corresponds to the experiment in [2] with no reshock.

3.1 Light Third Gas

For our first case, gas C is lighter than gas B (SF_6). The physical values of gas C correspond to helium, Table 1. When the shock reaches the first interface, it creates a transmitted and reflected shock. The transmitted shock impinges the second interface and creates another transmitted shock and a reflected rarefaction. The transmitted shock into gas C leaves the domain. The reflected rarefaction moves back towards the first interface and interacts with the evolving instability. This process initiates two RMIs with spikes moving in opposite directions: one into gas A and the other into gas C.

We show the growth of the RMI at the first interface for different non-dimensional spacings $\frac{h}{\lambda}$ between the first and third gases, Figure 3. Until the reflected rarefaction reaches this interface, the growth is that of the nominal case. This is followed by a transition regime where the growth is non-linear and increases dramatically. This is most likely due to the perturbed interface interacting with the rarefaction waves from the second interface. The third growth regime has a constant growth rate which increases with increasing $\frac{h}{\lambda}$. The increased growth and growth rate caused by the interaction with the rarefaction can be explained in the following way. The rarefaction deposits vorticity at the first interface in the same direction as the initial shock. Further amplifying growth, the rarefaction interacts with an evolving RMI so the perturbation amplitude is greater, Figure 4. Large values of $\frac{h}{\lambda}$ imply that the RMI has grown more and, therefore, the rarefaction increases the growth rate. The late-time morphology of the second interface is very different in the $\frac{h}{\lambda} = 0.5$ and $\frac{h}{\lambda} = 1$, Figures 4 and 5. Interface proximity effects might be affecting the flow dynamics at late times.

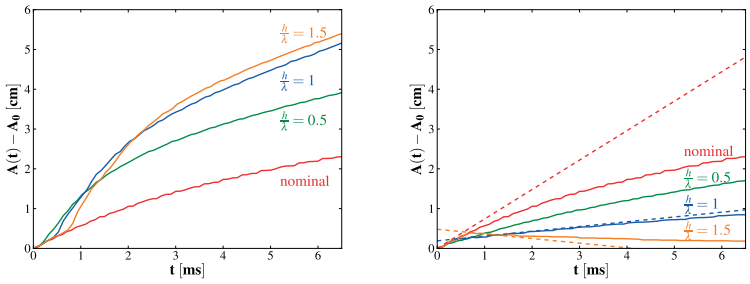

Fig. 3 Instability growth vs time. Left: case 1, right: case 2. Solid curves: simulation results. Dashed curves: linear theory [10]. All simulations at 128 cells per wavelength.

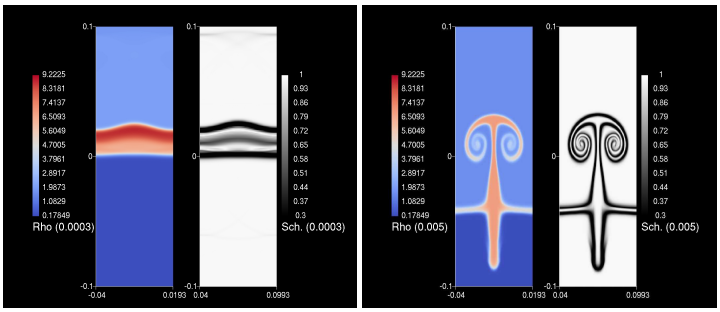

Fig. 4 Density and simulated Schlieren fields for case 1 and $\frac{h}{\lambda} = 0.5$ at $t = 0.3$ ms (right) and $t = 5$ ms (left).

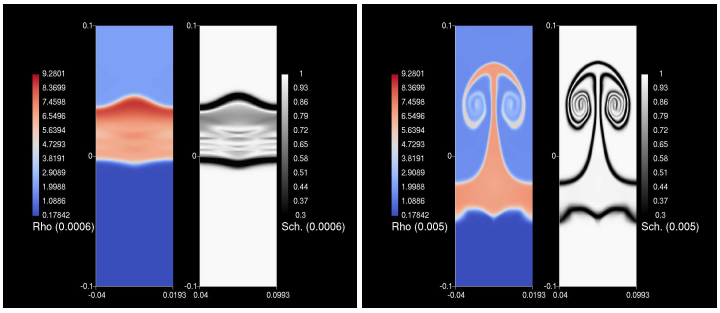

Fig. 5 Density and simulated Schlieren fields for case 1 and $\frac{h}{\lambda} = 1$ at $t = 0.6$ ms (right) and $t = 5$ ms (left).

3.2 Heavy Third Gas

The second case we analyze is that of a denser gas behind the SF_6, Table 1. In this case, the transmitted shock from the first interface creates a reflected and transmitted shock at the second interface. The reflected shock interacts with the evolving RMI

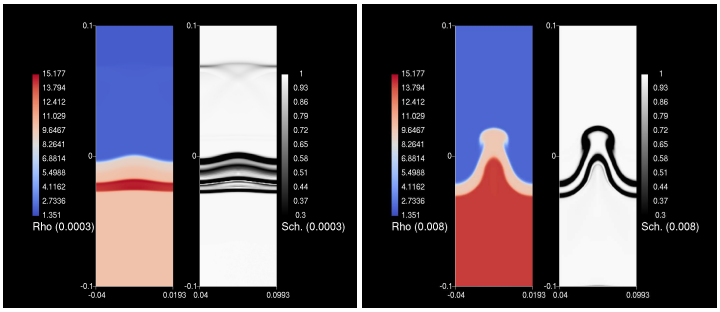

Fig. 6 Density and simulated Schlieren fields for case 2 and $\frac{h}{\lambda} = 0.5$ at $t = 0.3$ ms (right) and $t = 8$ ms (left).

at the first interface, Figure 6. Because of the setup, both RMIs grow in the same direction, with the first spike moving into gas A.

Figure 3 illustrates the growth of the RMI at the first interface for different $\frac{h}{\lambda}$. The RMI growth follows that of the nominal case until the reflected shock from the second interface reaches it. The growth and growth rate thereafter decrease as $\frac{h}{\lambda}$ increases. Because the reflected shock moves from a dense to a less dense gas, the reflected shock deposits vorticity in the opposite direction as the initial shock. This decreases the growth rate. Further amplifying this effect, the greater distance implies that the RMI has grown more before interacting with the reflected shock, Figures 6 and 7. As $\frac{h}{\lambda}$ increases, the growth rate becomes negative, indicating a phase reversal of the RMI. The perturbation amplitude does not increase dramatically as observed in experiments with reshock because the transmitted shock is much weaker and the interface is not that much more perturbed.

In Figure 3, we compare linear theory for the perturbation growth rate [10] to the initial growth rate of the instability and the growth rate after the interaction with the reflected shock. The linear theory growth rate equation is

$$\frac{\mathrm{d}a}{\mathrm{d}t} = k\Delta u A^{+} a_0^{+} \tag{1}$$

where $a(t)$ is the perturbation amplitude, a_0^+ is the post-shock amplitude, k is the perturbation wave number, $A^+ = (\rho_1^+ - \rho_2^+)/(\rho_1^+ + \rho_2^+)$ is the post-shock Atwood number, and Δu is the velocity jump at the interface following shock refraction. Linear theory seems to predict the correct initial growth rates after both shock interactions and deviates from the simulation results at later times.

4 Conclusions

In this work, we have shown the effect of the density of the third gas on the growth of the RMI at the first interface. If the third gas is lighter than the second gas, the

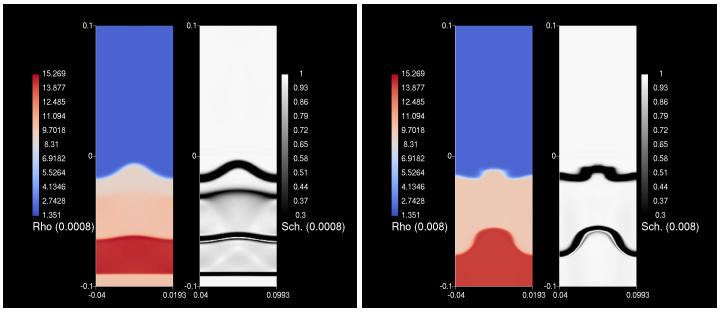

Fig. 7 Density and simulated Schlieren fields for case 2 and $\frac{h}{\lambda} = 1$ at $t = 0.8$ ms (right) and $t = 8$ ms (left).

reflected rarefaction at the second interface will amplify the growth at the first interface. If the third gas is heavier, the reflected shock will decrease the growth and tend to reverse the RMI as the thickness of the second gas increases. This study supports the idea that perturbation growth may be controlled using rarefactions and shocks [8]. This study will form the basis for considering additional quantities such as the time-evolution of vorticity and total kinetic energy and the transition to turbulence at late times. This research was supported by the DOE NNSA/ASC under the predictive Science Academic Alliance Program by Grant No. DEFC52-08NA28616.

References

1. Brouillette M., (2002) The Richtmyer-Meshkov instability. Ann. Rev. Fluid Mech. 34, 445468.
2. Collins B. D., Jacobs J. W. (2002). PLIF flow visualization and measurements of the Richtmyer-Meshkov instability of an air/SF6 interface. J. Fluid Mech. 464, 113136.
3. Drake R.P. (2006) High-Energy Density Physics, 1st Edition. Springer-Verlag, Berlin.
4. Henry de Frahan M.T., Johnsen E. (2012) Interface capturing for multifluid simulations with shocks using Discontinuous Galerkin approaches. Submitted.
5. Hill D. J., Pantano C., Pullin D. I. (2006) Large-eddy simulation and multiscale modelling of a Richtmyer-Meshkov instability with reshock. J. Fluid Mech. 557, 29-61.
6. Kifonidis K., Plewa T., Scheck L., Janka H. T., Muller E. (2006) Non-spherical core collapse supernovae - II. The late-time evolution of globally anisotropic neutrino-driven explosions and their implications for SN 1987 A. Astron. Astrophys. 453, 661678.
7. Latini M., Schilling O., Don W. S. (2007) Effects of WENO flux reconstruction order and spatial resolution on reshocked two-dimensional Richtmyer-Meshkov instability. J. Comput. Phys. 221, 805836.
8. Lindl J. (1995) Development of the indirect-drive approach to inertial confinement fusion and the target physics basis for ignition and gain. Phys. Plasmas 2, 39334024.
9. Movahed P., Johnsen E. (2013) A solution-adaptive method for efficient compressible multifluid simulations, with application to the Richtmyer-Meshkov instability. J. Comput. Phys. 239, 166-186.
10. Richtmyer, R. D. (1960) Taylor instability in shock acceleration of compressible fluids. Commun. Pure Appl. Math. 13, 297.